

# STUDY OF DIFFUSE NUV AND FUV RADIATION USING GALEX DEEP IMAGING SURVEYS

N.V. SUJATHA <sup>1</sup>, RAHUL SURESH <sup>2</sup>, JAYANT MURTHY <sup>1</sup>, R.C. HENRY <sup>3</sup> & LUCIANA BIANCHI <sup>3</sup>

<sup>1</sup> Indian Institute of Astrophysics, Bangalore

<sup>2</sup> National Institute of Technology Karnataka, India

<sup>3</sup> The Johns Hopkins University, Baltimore, USA

sujatha@iiap.res.in, rsbullz@gmail.com, murthy@iiap.res.in, rch@jhu.edu, bianchi@pha.jhu.edu

## INTRODUCTION

GALEX observations provide the highest spatial resolution images of the diffuse UV background, with an effective spatial resolution of about 5". 11 GALEX DIS observations were taken (Table. 1) both in FUV (1350-1750Å) and NUV (1750-2850Å) bands for the analysis of diffuse UV radiation from the GALEX archive. These targets are from an optically thin region. The dust map (Schlegel et al 1998) of the region and the GALEX field of view (1.26°) of the targets are shown in Fig. 1. E(B-V) variation in the field is 0.01 - 0.05 which corresponds to an optical depth of 0.0812 - 0.406.

Point sources were removed from each GALEX observation using the merged catalogue given in the archive to extract the diffuse signal. The signal to noise was increased by binning the image to 2' pixels which also enables us to remove unidentified faint sources from the field. Airglow, zodiacal light and dust scattered starlight are the 3 major components of the diffuse radiation. Method of extraction of these components are explained in detail in Sujatha et al. 2009.

Table.1: Details about the regions

| Tile_name  | RA_Cent | Dec_Cent | Nuv_ Exptime | Fuv_ Exptime | Fuv_ Visits | Nuv_ Visits |
|------------|---------|----------|--------------|--------------|-------------|-------------|
| SIRTFLL_00 | 259.11  | 59.91    | 52917.15     | 52016.95     | 39          | 41          |
| SIRTFLL_01 | 260.41  | 59.34    | 26006.1      | 30922.1      | 24          | 20          |
| SIRTFLL_02 | 260.09  | 58.5     | 39037.05     | 26859.35     | 25          | 30          |
| SIRTFLL_03 | 258.33  | 58.86    | 39830.4      | 29570.9      | 28          | 30          |
| SIRTFLL_04 | 256.98  | 59.72    | 3874.45      | 3874.45      | 3           | 3           |
| SIRTFLL_05 | 260.68  | 60.7     | 5305         | 5305         | 4           | 4           |
| SIRTFLL_06 | 257.58  | 60.45    | 27658.75     | 3668         | 9           | 22          |
| SIRTFLL_07 | 260.54  | 60.81    | 34376.55     | 21276.1      | 20          | 25          |
| SIRTFLL_08 | 262.61  | 59.15    | 40639.6      | 22540        | 20          | 28          |
| SIRTFLL_09 | 257.2   | 59.72    | 15737.4      | 3197.5       | 9           | 12          |
| SIRTFLL_10 | 256.99  | 58.8     | 27383.75     | 10757.7      | 15          | 21          |

## ERROR ANALYSIS

The visits of each observation are grouped into two sets to determine possible error in each observation. The results are tabulated in Table 2. The error in the FUV observations of SIRTFLL\_06 & 09 are very high compared to others because of the lack of enough good visits, which is also clear from its FUV-FUV correlation.

Table.2: Scatter in the observations

| Tile_name  | Scatter |       | Correlation - Coefficient |         |
|------------|---------|-------|---------------------------|---------|
|            | FUV     | NUV   | FUV-FUV                   | NUV-NUV |
| SIRTFLL_00 | 35.85   | 14.42 | 0.87                      | 0.95    |
| SIRTFLL_01 | 22.17   | 14.74 | 0.97                      | 0.95    |
| SIRTFLL_02 | 53.91   | 58.54 | 0.89                      | 0.87    |
| SIRTFLL_03 | 33.56   | 17.36 | 0.99                      | 0.97    |
| SIRTFLL_04 | 50.96   | 28.55 | 0.82                      | 0.82    |
| SIRTFLL_05 | 46.16   | 31.08 | 0.81                      | 0.72    |
| SIRTFLL_06 | 86.7*   | 16.07 | 0.67                      | 0.93    |
| SIRTFLL_07 | 36.41   | 22.89 | 0.85                      | 0.95    |
| SIRTFLL_08 | 32.4    | 22.52 | 0.89                      | 0.96    |
| SIRTFLL_09 | 161.47* | 18.68 | 0.41                      | 0.95    |
| SIRTFLL_10 | 42.78   | 11.31 | 0.97                      | 0.99    |

Table.4: Correlation between IR, NUV & FUV regions

| Tile_Name  | FUV-NUV Correlation | IR-FUV Correlation | IR-NUV Correlation |
|------------|---------------------|--------------------|--------------------|
| SIRTFLL_00 | 0.14                | 0.42               | -0.09              |
| SIRTFLL_01 | 0.61                | 0.73               | 0.62               |
| SIRTFLL_02 | 0.32                | 0.3                | 0.44               |
| SIRTFLL_03 | 0.85                | 0.92               | 0.82               |
| SIRTFLL_04 | 0.54                | 0.75               | 0.71               |
| SIRTFLL_05 | 0.29                | 0.18               | 0.37               |
| SIRTFLL_06 | 0.49                | 0.56               | 0.51               |
| SIRTFLL_07 | 0.34                | 0.4                | 0.52               |
| SIRTFLL_08 | 0.14                | 0.52               | 0.14               |
| SIRTFLL_09 | 0.31                | 0.35               | 0.5                |
| SIRTFLL_10 | 0.9                 | 0.93               | 0.87               |

## ABSTRACT

We present here preliminary results of the analysis of 11 GALEX DIS observations from nearby regions which are at medium latitude. We have estimated the error in the data of each of the observations from its visits. Different components of diffuse UV radiation were quantified and separated after removing the sources from each of the field. We then studied the dependencies of these components to factors such as solar activity, sun angle and Infrared 100 micron intensity, specific to each of these components.

Table.3: Airglow and Zodiacal Light values

| Tile_Name  | Sun Angle to LOS | Average FUV_AG | Average NUV_AG | $\lambda$ - $\lambda$ sun | $\beta$ | Average ZL | Correlation Coefficient  |                          |
|------------|------------------|----------------|----------------|---------------------------|---------|------------|--------------------------|--------------------------|
|            |                  |                |                |                           |         |            | Solar Flux - NUV_TEC_MIN | Solar Flux - FUV_TEC_MIN |
| SIRTFLL_00 | 89.17-95         | 238            | 243            | 84.17-128                 | 81.76   | 365        | 0.89                     | 0.68                     |
| SIRTFLL_01 | 90-98.2          | 131            | 136            | 90.67-193.5               | 81.59   | 367.3      | 0.81                     | 0.66                     |
| SIRTFLL_02 | 87.82-98.37      | 186            | 169            | 77-206.54                 | 80.76   | 372        | 0.98                     | 0.92                     |
| SIRTFLL_03 | 87.04-98.83      | 153            | 152            | 71.46-199                 | 80.67   | 381        | 0.98                     | 0.97                     |
| SIRTFLL_04 | 98.97-98.98      | 67             | 52             | 182.62-183.2              | 81.01   | 342        |                          |                          |
| SIRTFLL_05 | 97.07-97.11      | 91             | 48             | 187.47-190.2              | 82.84   | 342        | only 2 visits            |                          |
| SIRTFLL_06 | 90.08-98.07      | 132            | 123            | 92-195.65                 | 81.78   | 358        | 0.94                     |                          |
| SIRTFLL_07 | 87.01-96.73      | 202            | 141            | 65-201.2                  | 82.9    | 380        | 0.94                     | 0.85                     |
| SIRTFLL_08 | 89.37-97.74      | 145            | 152            | 86.3-163.1                | 81.87   | 363        | 0.92                     | 0.86                     |
| SIRTFLL_09 | 90.29-97.15      | 71             | 154            | 92.5-144.04               | 81.08   | 367        | 0.96                     | only 2 visits            |
| SIRTFLL_10 | 86.99-98.15      | 168            | 161            | 72.65-147.51              | 80.24   | 365        | 0.95                     | 0.61                     |

Fig.2a:

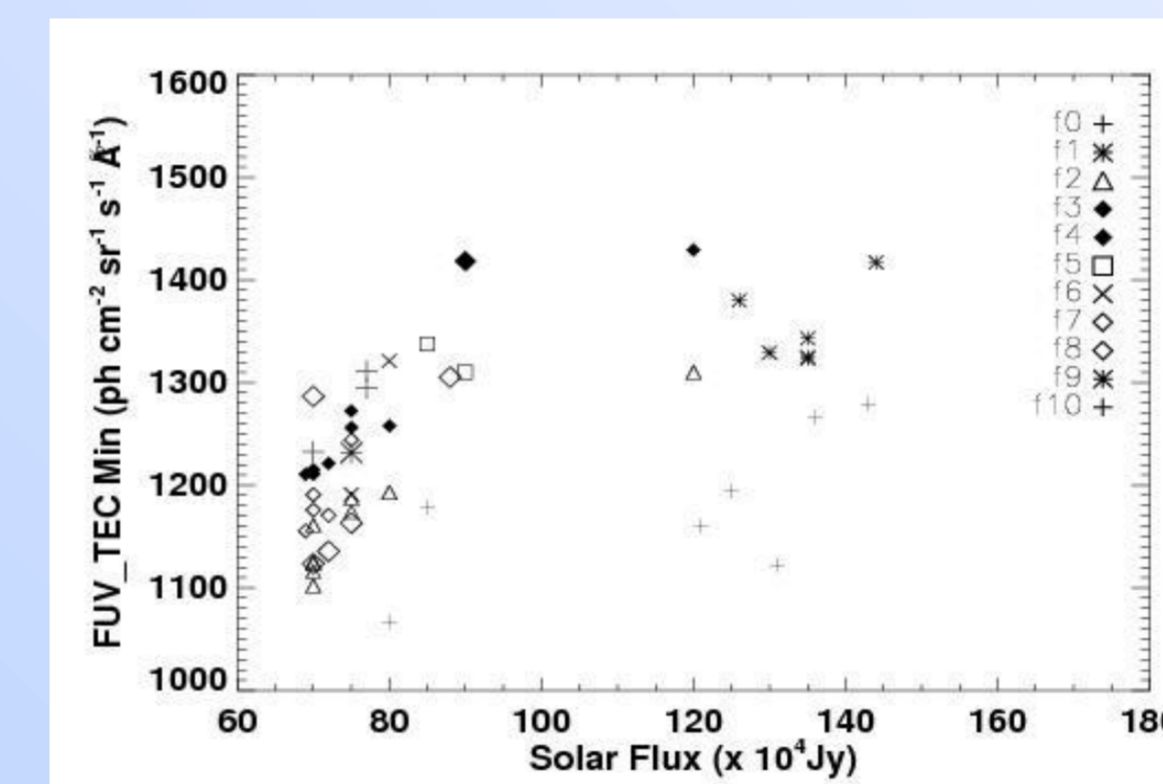
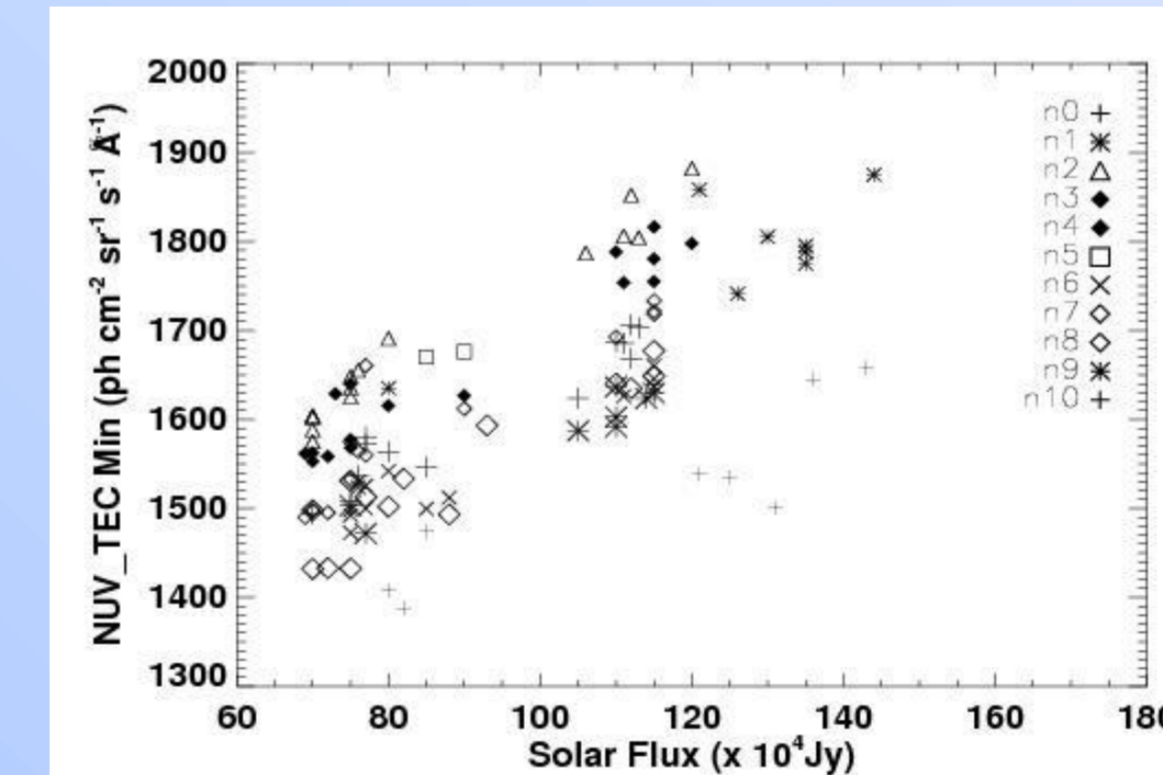


Fig.2b:



## AIRGLOW ESTIMATION AND SOLAR FLUX DEPENDENCE

Airglow is one of the major component of diffuse radiation in the field and is due to the resonantly scattered OI lines at 1304, 1356 and 2471 Å from the Earth's ionosphere. We extracted this component using the total count rate from the spacecraft state file of each visit assuming that the airglow contribution is negligible to the TEC\_MIN in the local midnight. The calculated values are tabulated in Table 2. We have also studied the variation of FUV & NUV TEC\_MIN with solar activity (Fig.2.). The airglow emission is dependent on the solar flux but perhaps not with a simple linear correlation. In our procedure, we estimate the level empirically from our data.

## ZODIACAL LIGHT CONTRIBUTION

Zodiacal light, is another major contributor in NUV images - which is sunlight scattered radiation from the interplanetary dust grains - is estimated for each observation from Leinert et al (1998) and tabulated in Table 3.

## CORRELATION STUDIES OF DIFFUSE UV RADIATION

We have studied the variation of total diffuse UV radiation relative to IR 100 micron intensity (Fig.3), which is a measure of interstellar dust grains in the region. In Fig. 3 and Fig. 4, we have plotted the entire signal observed in the data without subtracting the different components. Much of the scatter in the plots is due to the varying zodiacal light and airglow and the actual scatter (Table 2) is much less than shown. Fig. 4 is FUV - NUV correlation of 11 observations. The correlation details of FUV-NUV & IR-UV are given in Table.4.

Fig.3a

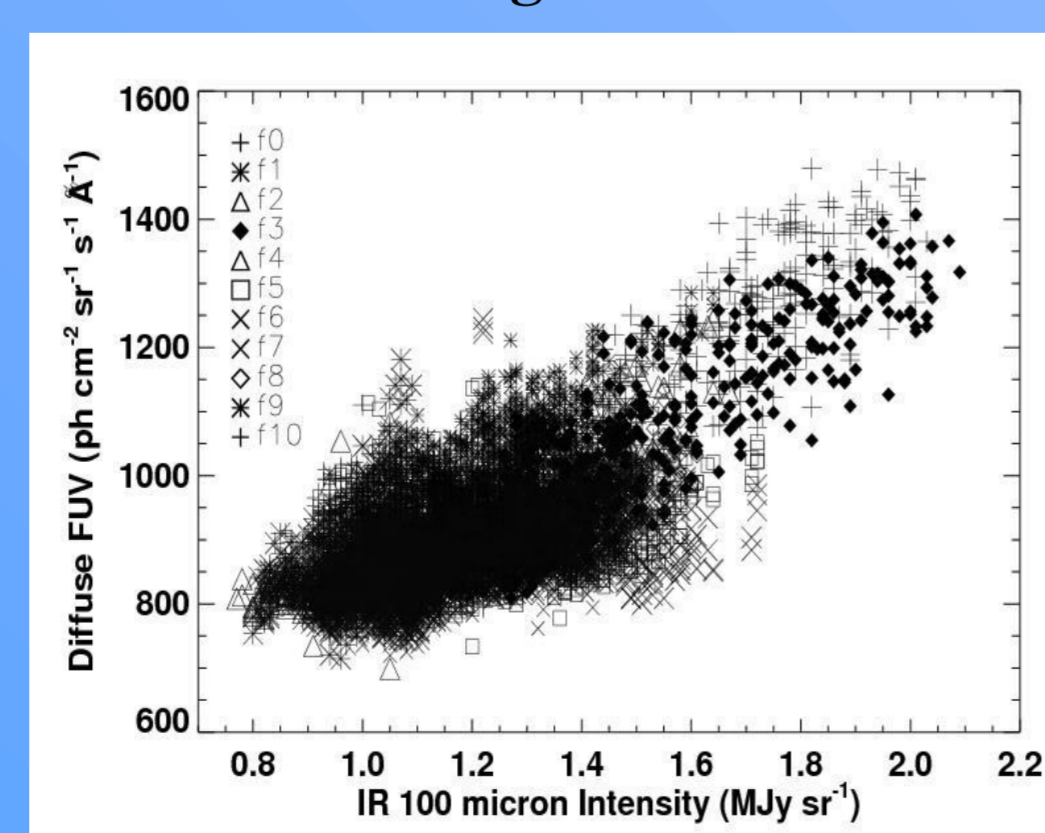


Fig.3b

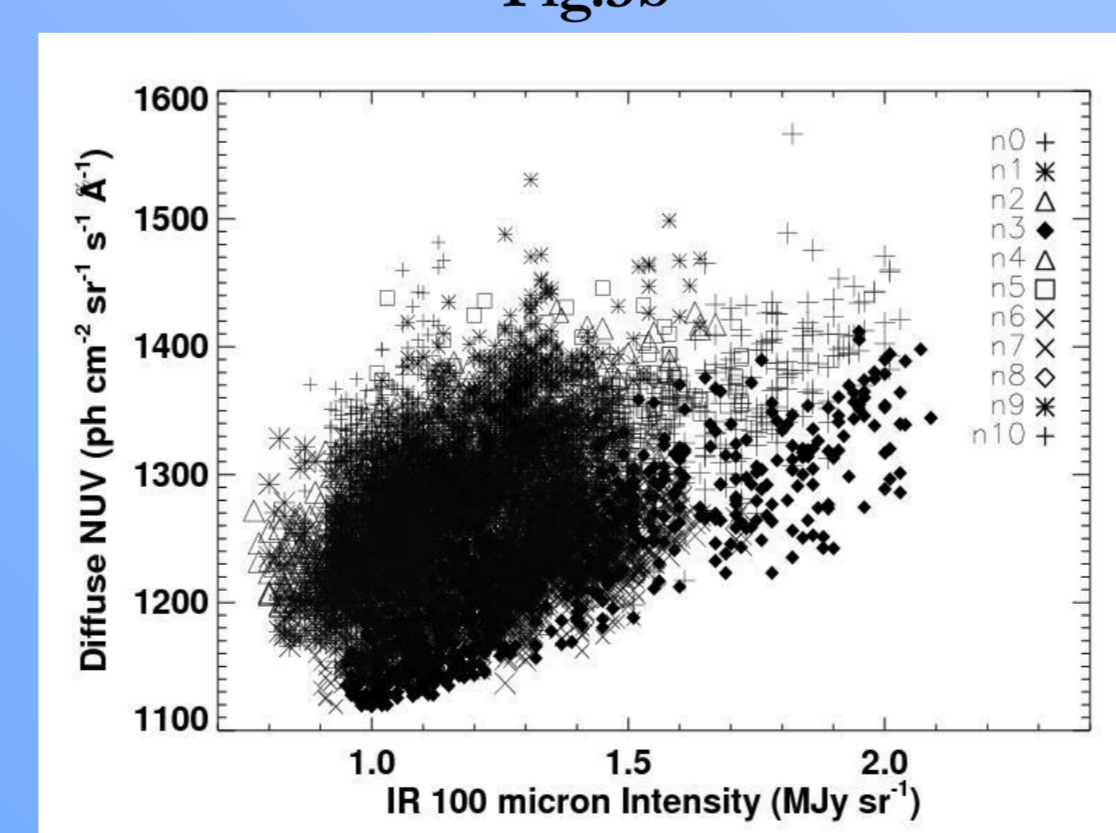
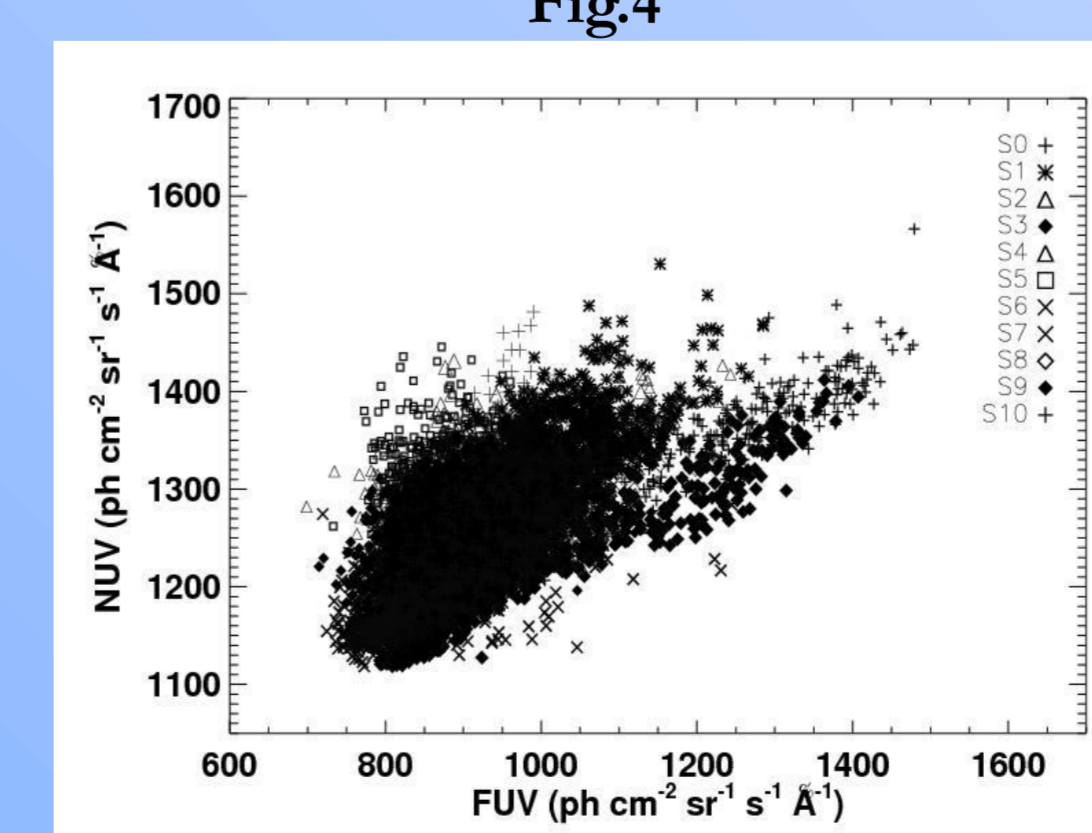


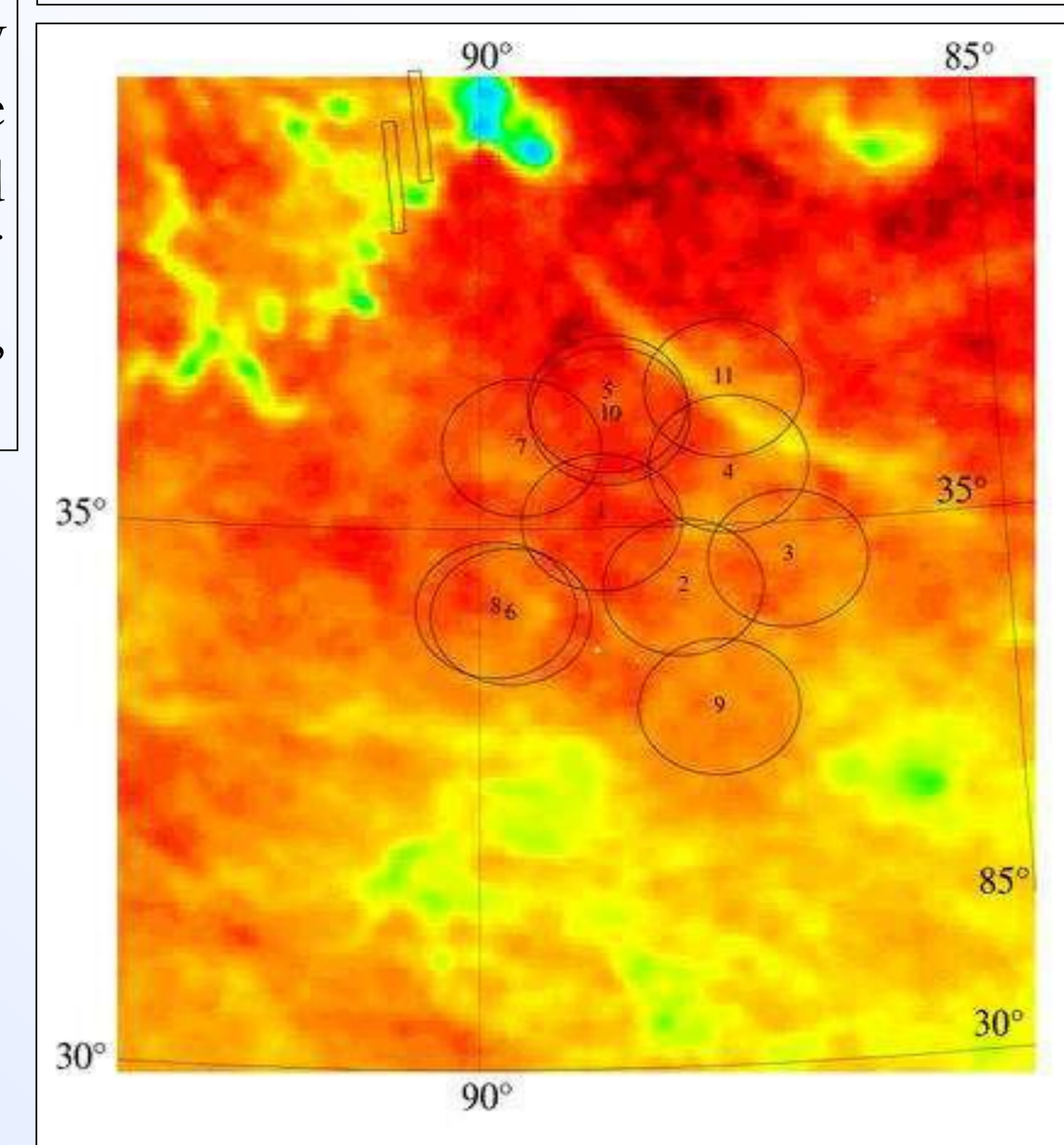
Fig.4



## REFERENCES

- [1] D. J. Schlegel, D.P. Finkbeiner, & M. Davis, ApJ, 500, 525.
- [2] N. V. Sujatha, J. Murthy, A. Karnataka, R. C. Henry, L. Bianchi, 2009, ApJ, Vol. No. 692 (in press): <http://arxiv.org/abs/0807.0189>
- [3] Leinert, C., et al. 1998, A&AS, 127, 1-99.

Fig.1: Schlegel's Dust-map for the region with GALEX FOV.



## RESULTS AND DISCUSSION

These observations are from an optically thin region. The data shows an intrinsic scatter which varies between 10 to 60 ph cm<sup>-2</sup> s<sup>-1</sup> sr<sup>-1</sup> Å<sup>-1</sup> both in FUV & NUV, much greater than what can be attributed to photon noise.

We observe that the airglow contribution empirically estimated from the data in the fields is very much depending on the solar activity at the time of observation, however not with a simple linear correlation. In our fields the average airglow contribution varies between 50 to 250 ph cm<sup>-2</sup> s<sup>-1</sup> sr<sup>-1</sup> Å<sup>-1</sup>.

We find that the total diffuse UV radiation increases linearly with the IR 100 micron intensity, which is from the entire volume of dust due to the low optical depth in the IR. We could also see that the FUV and NUV data in the observed regions are correlating well.

These are preliminary results of our analysis. In depth studies of the correlations we observed, extraction of dust scattered component in this radiation and the modeling of the same to extract the optical properties of dust grains in this region are underway.

## ACKNOWLEDGEMENT

N.V.S. is supported by a DST Young Scientist Award.